

allows interaction between X and the DKP ring without interference between X and Y. For the *cyclo*-(Y-Z) case where Y and Z are both L or D and are not aromatic, one can at least predict some kind of boat subject to Y-Z steric effects.

Acknowledgments. This work was begun with Research Corporation assistance and completed under National Science Foundation Grant No. GB-7376 and National Science Foundation Instrumentation Grant No. GP-10343. We are also grateful to Professors K. Kopple and G. Ramachandran and to Drs. A. Lakshminarayanan and R. Chandrasekaran for helpful discussions and computations. We are indebted to Mr.

B. Stevens for computational assistance. The molecular displays²⁹ were made possible by the Computer Systems Laboratory of Washington University Medical School and the kind assistance of Dr. J. M. Fritsch.

Supplementary Material Available. Observed and calculated structure factors for *cyclo*-(Gly-L-Tyr) and *cyclo*-(L-Ser-L-Tyr) will appear following these pages in the microfilm edition of this volume of the journal. Photocopies of the supplementary material from this paper only or microfiche (105 × 148 mm, 20× reduction, negatives) containing all of the supplementary material for the papers in this issue may be obtained from the Journals Department, American Chemical Society, 1155 16th St., N.W., Washington, D. C. 20036. Remit check or money order for \$7.00 for photocopy or \$2.00 for microfiche, referring to code number JACS-73-6803.

Structure of Copper(II) *n*-Propylporphine. Effect of a Metallo Substitution on the Free Base Macrocycle

Irene Moustakali and A. Tulinsky*

Contribution from the Departments of Chemistry and Biochemistry, Michigan State University, East Lansing, Michigan 48823.

Received March 14, 1973

Abstract: The crystal and molecular structure of copper(II) $\alpha,\beta,\gamma,\delta$ -tetra-*n*-propylporphine has been determined by X-ray crystallographic methods. The compound crystallizes in the space group $P2_1/c$ with two molecules per unit cell of dimensions $a = 5.010$ (7), $b = 11.55$ (4), $c = 22.50$ (9) Å, $\beta = 99.1$ (2)°. The metallo structure is isomorphous with the free base and it was solved from a sharpened, three-dimensional Patterson function. The structure was refined by full-matrix, least-squares procedures with the final *R* factor being 0.059 ($R = \sum ||F_o| - |F_c|| / \sum |F_o|$). The molecule is centrosymmetric with half of a molecule per asymmetric unit. The two independent pyrrole rings have very similar bond distances and bond angles and have the geometry of the azapyrrole of the free base structure. This gives the macrocycle a symmetry closely approaching D_{4h} . The Cu(II) ion substitution causes a general "squaring-up" and overall contraction of the central core region of the free base macrocycle. This is accomplished by the movement of the pyrrole rings. The individual pyrrole rings are planar to ± 0.004 Å whereas the porphine macrocycle is only planar to ± 0.05 Å. In the case of the latter, the pyrroles are tilted slightly with respect to each other (3.7°).

Among other derivatives in our continuing study of the structures of porphyrin molecules, we have been interested in determining the effect of a metallo substitution upon the porphine macrocycle when the substitution was expected intrinsically to lead only to minor perturbations of the original system. With the recent advent of a precise description of the geometry of the free base macrocycle,¹ such a plan became feasible. Therefore, to this end, we have focused our attention upon the Cu(II) state. The ionic radius of Cu(II) was expected to be nearly optimal for undistorted accommodation within the central porphine core;² moreover, the ion favors square planar coordination and this should minimize geometrical perturbations on the macrocyclic system with substitution. In this way, we hoped to isolate the effect of chemical bond formation from other extraneous factors and to establish a base from which more complicated metallo substitutions might be better understood (different ionic radii, different electronic spin states, more complicated coordination geometries).³

(1) P. W. Codding and A. Tulinsky, *J. Amer. Chem. Soc.*, **94**, 4151 (1972).

(2) J. L. Hoard, *Science*, **174**, 1295 (1971).

Experimental Section

Twinned crystals of copper $\alpha,\beta,\gamma,\delta$ -tetra-*n*-propylporphine (CuTPrP)⁴ in the form of purple needles were prepared by allowing methanol to diffuse into a saturated solution of the compound in toluene. Various other solvents and other conditions also gave twinned crystals in the form of hexagonal prisms. However, some of these crystals could be cleaved into two nontwinned crystal fragments. A suitable nontwinned crystal fragment with approximate dimensions 0.05 × 0.075 × 0.5 mm was used for the X-ray studies.

Preliminary X-ray diffraction measurements showed the crystal system to be monoclinic and systematic absences of reflections showed the space group to be $P2_1/c$. The lattice parameters were obtained from diffractometer measurements by the least-squares fit of the angular coordinates of 12 reflections in the range $45^\circ < 2\theta < 80^\circ$ [$a = 5.010$ (7), $b = 11.55$ (4), $c = 22.50$ (9) Å and $\beta = 99.1$ (2)°]. The calculated density of the crystal on the basis of two molecules per unit cell is 1.396 g cm⁻³ and the observed density measured by flotation in aqueous silver nitrate solution is 1.39 g cm⁻³.

The intensity data collection was carried out with Cu K α radiation using a Picker four-circle diffractometer controlled by a Digital Equipment Corp. (DEC) 4K PDP-8 computer (FACS-I system)

(3) E.g., square pyramidal chloromanganese tetraphenylporphine; B. M. L. Chen, Ph.D. Thesis, Michigan State University, 1970.

(4) We would like to thank Dr. Alan D. Adler of the New England Institute, for kindly supplying us with a sample of CuTPrP.

coupled to a DEC 32K disc file and an Ampex TMZ 7-track tape transport. Intensities of reflections were measured by a wandering ω -step-scan procedure using balanced Ni/Co filters.⁵ The step-scan was performed in 0.03° increments of the ω angle and extended $\pm 0.075^\circ$ on either side of the calculated peak position. Each step was measured for a duration of 4 sec and the four largest measurements were summed to give the intensity of the reflection.⁶ When the observed peak position did not coincide with the calculated ω value, one or two additional steps were taken to assure centering of the scan in the detector window. The background was measured with a Co filter at the ω value of the maximum intensity for a time interval of 4 sec and this count was multiplied by four to give the total background intensity. Finally, since the step-scan procedure is essentially a stationary crystal-stationary counter measurement, in order to avoid $K\alpha$ splitting effects, the intensity data collection was confined within the range $2\theta < 115^\circ$.

During the intensity data collection the alignment of the crystal was monitored by measuring the intensities of three standard reflections. These standard reflections were the $(\bar{2}00)$ at $\chi = 90^\circ$ and two φ values approximately 90° apart and the $(0\bar{6}4)$ reflection. The program which controlled the intensity data collection also had the capability of "realigning" the crystal automatically.⁵ The need for realignment is based on the intensities of the standard reflections but since the deviations of the standards were all within the counting statistics, no realignment occurred during the data collection. Before the onset of intensity data collection, the mosaic spreads of two reflections were measured to ensure the crystal quality and to help select the best quadrant to be used for the intensity data collection. A quadrant including the $-b^*$ axis was selected where the peak widths were generally smaller ($< 0.3^\circ$) and the absorption by the crystal was less.

The intensities of the reflections were corrected for absorption using a semiempirical method based on the variation of the relative transmission (T) with the azimuthal angle φ .⁷ The $T(\varphi)$ curves were constructed by measuring the variation of the absorption of reflections at $\chi = 90^\circ$. Since the $-a^*$ axis occurred at $\varphi = 90^\circ$, the $(\bar{h}00)$ reflections were used to correct general reflections for absorption in terms of φ , 2θ , and reciprocal lattice level (h index). The absorptions measured were of the reflections: $(\bar{1}00)$, $(\bar{2}00)$ and $(\bar{3}00)$ with $2\theta = 17.9$, 36.3 , and 55.7° , respectively. The maxima of the absorption ratios of these reflections occurred at the $\pm b^*$ directions. The intensities of a total of 1885 independent reflections were measured of which 591 were taken to be accidentally absent. The observable limit was fixed by the average value of the measured intensity of the systematically absent ($h0l$) reflections (~ 1 count/sec) (1294 observable reflections or 69%). The intensities were then converted to relative structure amplitudes by application of the Lorentz and polarization factors.

Structure Analysis

The structure amplitudes were converted to normalized values using an approximate scale and an average isotropic temperature factor (3.0 \AA^2) determined by Wilson's method.⁸ Since the crystal density shows that there are two molecules per unit cell and the space group requires four equivalent positions, two related by centers of symmetry, the molecules must be centrosymmetrical with the Cu(II) ions located at the centers of symmetry. A sharpened, origin removed, three-dimensional Patterson ($|E^2 - 1|$) map showed the image of the molecule clearly centered around the origin.

The coordinates of the nonhydrogen atoms were measured from the Patterson map and were used to start the refinement process. The initial coordinates and an average isotropic thermal parameter gave $R = 0.24$, $R = \sum ||F_o| - |F_c|| / \sum |F_o|$, where $|F_o|$ and $|F_c|$

(5) R. L. Vandlen and A. Tulinsky, *Acta Crystallogr., Sect. B*, **27**, 437 (1971).

(6) H. W. Wyckoff, M. Doscher, D. Tsernoglou, T. Inagami, L. N. Johnson, K. D. Hardman, N. M. Allewell, D. M. Kelly, and F. M. Richards, *J. Mol. Biol.*, **27**, 563 (1967).

(7) A. C. T. North, D. C. Phillips, and F. S. Mathews, *Acta Crystallogr., Sect. A*, **24**, 351 (1968).

(8) A. J. C. Wilson, *Nature (London)*, **150**, 151 (1942).

are the observed and calculated structure amplitudes, respectively.

The structure was refined using full-matrix, least-squares methods with unit weights applied to the structure amplitudes. Three cycles of refinement, one varying the positional parameters of the atoms, another varying isotropic temperature factors, and the last varying the positional parameters again along with the scale of the observed amplitudes, lowered R to 0.102. At this stage, a difference electron density map was calculated and it revealed the positions of all the hydrogen atoms. The hydrogen atoms were assigned isotropic temperature factors which were 1.25 greater than the isotropic temperature factors of the carbon atoms to which they were bonded and the resulting structure factor calculation had an R of 0.086. Anisotropic thermal parameters were introduced at this stage and the course of the remainder of the refinement is summarized in Table I. In Table I, k is the absolute

Table I. Summary of the Refinement with Anisotropic Thermal Parameters

Cycle	k	$(xyz)_j$	β_{ij}	$(xyz)_H$	R
1					0.086
2			X		0.072
3		X			0.068
4				X	0.065
5		X			0.064
6	X		X		0.062
7		X			0.062
Second difference map, new $(xyz)_H$					
8				X	0.062
9		X	X		0.062
Introduced Cu atomic scattering factor dispersion correction increasing R to 0.104					
10			β_{ij} of Cu only		0.067
11	X	X			0.065
12			X		0.063
Introduced 2θ dependence in absorption (two absorption curves), increasing R to 0.065					
13	X	X			0.061
14			X		0.060
15		X	X		0.059
Third difference map, new $(xyz)_H$					
16		X			0.059
17			X		0.059
18				X	0.059

scale factor of the observed structure amplitudes, $(xyz)_j$ represents the atomic coordinates of the nonhydrogen atoms, β_{ij} represents the anisotropic thermal parameters of these atoms, and $(xyz)_H$ corresponds to the hydrogen atom coordinates. An X in Table I denotes the parameters which were varied during a particular least-squares cycle.

Results⁹

The final atomic parameters of the nonhydrogen atoms are listed in Table II and Table III lists the equivalents of the principal mean-square displacements of the atoms. The atom notation is according to Figure 1. The hydrogen atomic coordinates and isotropic temperature factors are listed in Table IV. The interatomic bond distances and bond angles of

(9) See paragraph at end of paper regarding supplementary material.

Table II. Final Atomic Parameters^a

Atom	<i>x</i>	<i>y</i>	<i>z</i>	β_{11}	β_{22}	β_{33}	β_{12}	β_{13}	β_{23}	Peak height, e Å ⁻³
Cu	0	0	0	0.0344	0.0068	0.0014	0.0005	0.0007	0.00009	48.0
N(A)	0.2255 (9)	0.0193 (4)	-0.0648 (2)	0.0387	0.0068	0.0015	0.0004	0.0008	-0.00012	7.2
C(A1)	0.2552 (12)	0.1177 (6)	-0.0975 (3)	0.0380	0.0082	0.0016	-0.0015	0.0005	0.00026	5.9
C(A2)	0.4409 (13)	0.0961 (6)	-0.1394 (3)	0.0503	0.0090	0.0020	-0.0021	0.0032	-0.00026	5.4
C(A3)	0.5253 (12)	-0.0141 (6)	-0.1313 (3)	0.0447	0.0108	0.0017	-0.0020	0.0027	-0.00073	5.6
C(A4)	0.3910 (12)	-0.0631 (5)	-0.0847 (3)	0.0381	0.0077	0.0016	0.0000	0.0006	-0.00049	6.2
C(M5)	0.4238 (12)	-0.1773 (6)	-0.0654 (3)	0.0335	0.0083	0.0017	0.0004	0.0006	-0.00081	5.8
C(P51)	0.6088 (12)	-0.2554 (6)	-0.0945 (3)	0.0383	0.0090	0.0019	0.0034	0.0008	-0.00056	5.4
C(P52)	0.4613 (13)	-0.3151 (6)	-0.1515 (3)	0.0490	0.0090	0.0022	0.0002	0.0014	-0.00119	5.5
C(P53)	0.6549 (16)	-0.3903 (7)	-0.1811 (3)	0.0724	0.0090	0.0030	0.0021	0.0044	-0.00118	4.7
N(B)	0.1155 (10)	-0.1659 (4)	0.0098 (2)	0.0386	0.0074	0.0014	0.0020	0.0004	0.00017	7.3
C(B1)	0.2887 (12)	-0.2237 (6)	-0.0213 (3)	0.0361	0.0078	0.0018	0.0010	-0.0001	-0.00033	5.7
C(B2)	0.3086 (14)	-0.3438 (6)	-0.0029 (3)	0.0526	0.0086	0.0020	0.0039	0.0020	0.00015	5.7
C(B3)	0.1540 (15)	-0.3568 (6)	0.0403 (3)	0.0602	0.0070	0.0024	0.0043	0.0008	0.00056	5.3
C(B4)	0.0323 (12)	-0.2457 (6)	0.0495 (3)	0.0427	0.0076	0.0017	0.0006	-0.0005	0.00001	6.0
C(M6)	-0.1347 (12)	-0.2243 (6)	0.0916 (3)	0.0401	0.0077	0.0017	-0.0010	0.0008	0.00047	6.3
C(P61)	-0.1848 (14)	-0.3191 (6)	0.1346 (3)	0.0504	0.0083	0.0020	-0.0027	0.0015	0.00041	5.8
C(P62)	-0.0004 (14)	-0.3120 (6)	0.1950 (3)	0.0534	0.0092	0.0018	-0.0023	0.0008	0.00071	5.6
C(P63)	-0.0843 (15)	-0.3937 (7)	0.2415 (3)	0.0642	0.0107	0.0025	-0.0012	0.0026	0.00159	4.8
$\sigma \times 10^5$	93-158	42-66	19-34	50-463	10-77	2-21	24-155	8-78	5-32	

^a Anisotropic temperature factor = $\exp[-(\beta_{11}h^2 + \beta_{22}k^2 + \beta_{33}l^2 + 2\beta_{12}hk + 2\beta_{13}hl + 2\beta_{23}kl)]$. Standard deviations of coordinates in parentheses.

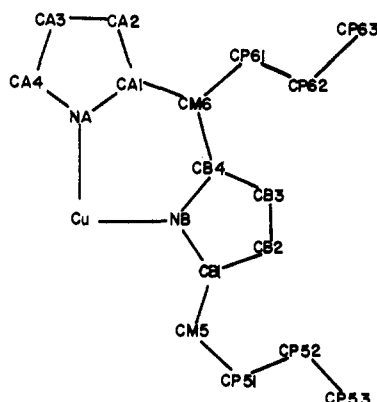


Figure 1. Numbering system of CuTPrP.

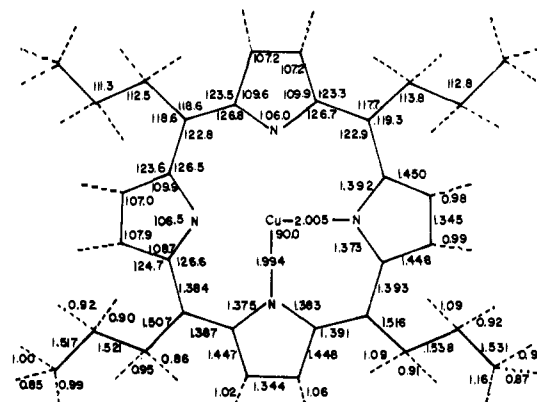


Figure 2. Interatomic distances (Å) and bond angles (deg) of CuTPrP.

Table III. Principal Mean-Square Displacements (Å²) in "Isotropic B" Notation

	$8\pi^2\bar{\mu}_1^2$	$8\pi^2\bar{\mu}_2^2$	$8\pi^2\bar{\mu}_3^2$
Cu	2.76	3.38	3.72
N(A)	2.98	3.57	3.92
C(A1)	2.98	3.64	4.66
C(A2)	3.42	4.47	5.56
C(A3)	2.96	4.28	6.14
C(A4)	2.86	3.80	4.38
C(M5)	2.83	3.32	4.94
C(P51)	3.27	3.52	5.52
C(P52)	3.40	4.79	5.93
C(P53)	3.62	6.43	7.48
N(B)	2.63	3.59	4.37
C(B1)	3.00	3.76	4.64
C(B2)	3.91	4.00	5.80
C(B3)	3.13	4.95	6.40
C(B4)	2.92	4.25	4.86
C(M6)	3.06	3.78	4.54
C(P61)	3.56	4.30	5.46
C(P62)	3.24	4.61	5.98
C(P63)	3.55	6.30	7.09

CuTPrP are shown in Figure 2. For comparison, Figure 3 shows the interatomic distances and angles of TPrP. The standard deviations of the nonhydrogen

Table IV. Final Hydrogen Atom Parameters

Atom	<i>x</i>	<i>y</i>	<i>z</i>	Isotropic <i>B</i> , Å ²	Peak height, e Å ⁻³
HCA2	0.4951	0.1510	-0.1711	4.8	0.39
HCA3	0.6849	-0.0528	-0.1496	5.3	0.45
H1P51	0.7793	-0.2070	-0.1063	4.6	0.46
H2P51	0.6908	-0.3057	-0.0663	4.6	0.53
H1P52	0.3754	-0.2544	-0.1865	5.0	0.40
H2P52	0.3160	-0.3610	-0.1464	5.0	0.41
H1P53	0.7855	-0.3392	-0.1903	5.8	0.37
H2P53	0.7196	-0.4451	-0.1564	5.8	0.38
H3P53	0.5429	-0.4335	-0.2249	5.8	0.37
HCB2	0.4403	-0.4007	-0.0142	4.9	0.47
HCB3	0.1355	-0.4249	0.0650	5.1	0.38
H1P61	-0.3487	-0.3180	0.1412	4.8	0.40
H2P61	-0.1623	-0.3946	0.1188	4.8	0.49
H1P62	0.0083	-0.2379	0.2078	4.8	0.45
H2P62	0.1749	-0.3215	0.1880	4.8	0.42
H1P63	0.0382	-0.3896	0.2810	5.9	0.49
H2P63	-0.0777	-0.4624	0.2288	5.9	0.34
H3P63	-0.2763	-0.3756	0.2429	5.9	0.27
$\sigma \times 10^4$	133-154	60-68	29-34		

bond distances and angles are about ± 0.008 Å and 0.55° , respectively. These are based on the standard

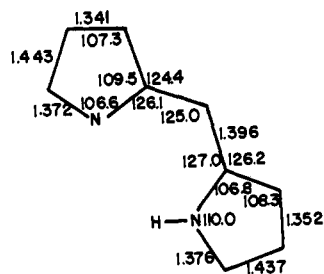


Figure 3. Average interatomic distances (Å) and bond angles (deg) of independent pyrroles of TPrP.

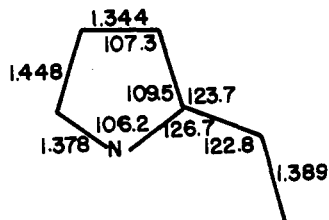


Figure 4. Average interatomic distances (Å) and bond angles (deg) of independent pyrroles of CuTPrP.

deviations of the atomic coordinates of the final cycle of least-squares refinement (shown in parentheses in Table II). The errors in the hydrogen atom coordinates are about ten times greater than those of the atom to which they are bonded.

A least-squares plane was calculated for the atoms of the porphine skeleton. The deviations of the atoms from the least-squares plane are listed in Table V.

Table V. Deviations of the Atoms of the Porphine Skeleton from the Best Least-Squares Plane

Atom	δ , Å	Atom	δ , Å
N(A)	-0.02	N(B)	0.01
C(A1)	-0.04	C(B1)	0.02
C(A2)	-0.02	C(B2)	-0.04
C(A3)	0.03	C(B3)	-0.05
C(A4)	0.03	C(B4)	0.00
C(M5)	0.04	C(M6)	0.05
$\sigma = \pm 0.03$ Å			

Best least-squares planes were also computed for the atoms of each pyrrole ring separately. The pyrroles are planar within ± 0.004 Å (Table VI) but the por-

Table VI. Deviations of the Atoms of the Pyrroles from Best Least-Squares Planes

Pyrrole A		Pyrrole B	
Atom	δ , Å	Atom	δ , Å
N(A)	-0.004	N(B)	-0.013
C(A1)	0.004	C(B1)	0.011
C(A2)	-0.003	C(B2)	-0.005
C(A3)	0.000	C(B3)	-0.003
C(A4)	0.003	C(B4)	0.010
$\sigma = \pm 0.002$ Å		$\sigma = \pm 0.005$ Å	

phine macrocycle is only planar to within ± 0.05 Å; in the latter, the pyrroles are tilted with respect to each other by an angle of 3.7° .

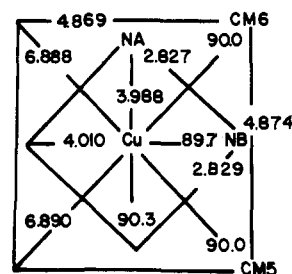
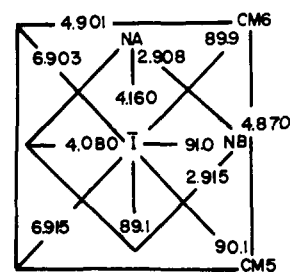


Figure 5. Comparison of central core region of TPrP (top) and CuTPrP (bottom).

Discussion

Since the porphine macrocycle of CuTPrP is essentially planar and since the geometry of the independent pyrroles is practically identical (Figure 2), the porphine skeleton closely approximates D_{4h} symmetry. Furthermore, from a comparison of the bond distances and especially from the bond angles of CuTPrP and its free base counterpart (Figures 2 and 3), it can be seen that *the reduced pyrrole of the free base assumes the geometry of the azapyrrole upon the loss of hydrogen atoms and concomitant coordination and bond formation with the Cu(II) ion*. Although the D_{4h} symmetry was expected, the same is not necessarily so concerning the manner in which the symmetry was achieved, since there are a number of likely *a priori* ways to establish the D_{4h} symmetry. The average bond distances and bond angles of CuTPrP corresponding to D_{4h} symmetry are shown in Figure 4.

The foregoing results agree well with the triclinic structure determinations of octaethylporphine (OEP)¹⁰ and NiOEP.¹¹ The OEP macrocycle is similar to the average free base structure of the porphine macrocycle¹ except in the vicinity of the ethyl group substitutions. A similar phenomenon was noted in the vicinity of the propyl and phenyl substitutions of TPrP and tetraphenylporphine.¹ The NiOEP structure closely approximates D_{4h} symmetry and the pyrroles assume the geometry of the azapyrrole of the free base of OEP, similarly to that just described for CuTPrP and TPrP.

The distances between the methine carbon atoms, which possess good square symmetry in TPrP, do not change much with the Cu(II) substitution (~ 0.02 Å). However, the bond angles involving the methine carbon atoms decrease by about 2.2° from the movement of the pyrroles toward the Cu(II) ion giving rise

(10) J. W. Lauher and J. A. Ibers, Abstracts, Winter Meeting of the American Crystallographic Association, Gainesville, Fla., January 1973, A2.

(11) D. L. Cullen and E. F. Meyer, Jr., Abstracts, Winter Meeting of the American Crystallographic Association, Gainesville, Fla., January 1973, A1.

to an overall contraction of the central core region. This can be seen from Figure 5 which compares the geometry of the central core region of TPrP and CuTPrP. From Figure 5, it can be seen that in CuTPrP the arrangement of the pyrrolic nitrogen atoms "square-up" with an accompanying overall contraction (average ~ 0.12 Å). Since the central core radius of 2.01 Å corresponds to the minimization of radial strain in the porphine macrocycle of a metalloporphine,² the observed value of 2.000 ± 0.005 Å in CuTPrP would seem to suggest that the Cu(II) ion is accommodated with a minimal perturbation to the system. A similar but more pronounced contraction of the central core region is observed with NiOEP.¹²

The bond distances of the propyl groups are not affected by the Cu(II) substitution. As in TPrP, the distances tend to be smaller than expected (second and third atoms of the side chains). In fact, the distribu-

(12) D. L. Cullen and E. F. Meyer, Jr., private communication.

tions of the bond distances in the propyl groups of TPrP and CuTPrP are remarkably similar. Since the structures are isomorphous, this reproducibility would seem to suggest that the shortening in some of these distances might be related to packing effects noted in the TPrP structure (close intermolecular contacts).¹

Acknowledgment. We would like to take the opportunity here to gratefully acknowledge the support of this work by the National Science Foundation, Molecular Biology Section (Grant No. GB-3372XX).

Supplementary Material Available. A table of $|F_o|$ and F_c (in electrons) will appear following these pages in the microfilm edition of this volume of the journal. Photocopies of the supplementary material from this paper only or microfiche (105 × 148 mm, 20× reduction, negatives) containing all of the supplementary material for the papers in this issue may be obtained from the Journals Department, American Chemical Society, 1155 16th St., N.W., Washington, D. C. 20036. Remit check or money order for \$3.00 for photocopy or \$2.00 for microfiche, referring to code number JACS-73-6811.

Studies on Polypeptides. LII. Synthesis of a Cysteine Protected Peptide Amide Corresponding to Positions 81–104 of the Ribonuclease T₁ Sequence^{1–3}

Koichi Kawasaki, Roger Camble, Gilles Dupuis, Hana Romovacek, Harold T. Storey, Chizuko Yanaiharu, and Klaus Hofmann*

Contribution from the Protein Research Laboratory, University of Pittsburgh, School of Medicine, Pittsburgh, Pennsylvania 15261. Received May 9, 1973

Abstract: Syntheses are described of a cysteine protected tetracosapeptide amide which corresponds to positions 81–104 of the proposed primary sequence of the enzyme ribonuclease T₁. The peptide amide was constructed by the protected hydrazide approach and was shown to be sequentially homogeneous. The low solubility of the tetracosapeptide and several subfragments used in its synthesis created problems as concerns purification and these are discussed. Some racemization may have occurred during formation of the phenylalanyl–valine bond, but its level was below that detectable by enzymatic digestion.

We have reported syntheses of two protected peptide hydrazides corresponding to positions 1–47 (fragment ABCD)¹ and 48–80 (fragment EF)⁴ of the proposed amino acid sequence of the enzyme

(1) See H. T. Storey, J. Beacham, S. F. Cernosek, F. M. Finn, C. Yanaiharu, and K. Hofmann, *J. Amer. Chem. Soc.*, **94**, 6170 (1972), for paper LI in this series. A preliminary communication of some of the results presented in this paper has appeared: N. Yanaiharu, C. Yanaiharu, G. Dupuis, J. Beacham, R. Camble, and K. Hofmann, *ibid.*, **91**, 2184 (1969).

(2) Supported by grants from the U. S. Public Health Service, the National Science Foundation, and the Hoffmann-La Roche Foundation.

(3) The amino acid residues except glycine are of the L configuration. The following abbreviations are used: AP-M = aminopeptidase M [G. Pfeiderer, P. G. Celliers, M. Stanulovic, E. D. Wachsmuth, H. Determann, and G. Braunitzer, *Biochem. Z.*, **340**, 552 (1964)]; Boc = *tert*-butoxycarbonyl; DCC = *N,N'*-dicyclohexylcarbodiimide; DCU = *N,N'*-dicyclohexylurea; DMSO = dimethyl sulfoxide; DMF = dimethylformamide; EC = ethylcarbonyl; EtOH = ethanol; F = formyl; HOSU = *N*-hydroxysuccinimide; MeOH = methanol; OCP = 2,4,5-trichlorophenyl ester; ONHS = *N*-hydroxysuccinimido ester; *O-t*-Bu = *tert*-butyl ester; TEA = triethylamine; TFA = trifluoroacetic acid; THF = tetrahydrofuran; tlc = thin-layer chromatography; X = *tert*-butoxycarbonylhydrazide; Z = benzyl-oxy-carbonyl. See ref 1 for nomenclature of complex peptide derivatives.

(4) R. Camble, G. Dupuis, K. Kawasaki, H. Romovacek, N. Yanaiharu, and K. Hofmann, *J. Amer. Chem. Soc.*, **94**, 2091 (1972).

ribonuclease T₁ (ribonuclease guanine nucleotido-2'-transferase (cyclizing) 2.7.7.26).⁵ Our fundamental studies on fragment condensation have been continued and the present communication describes experimental details for the preparation of a cysteine protected tetracosapeptide amide (fragment G) corresponding to positions 81–104 of the enzyme's peptide chain. The synthesis of three large fragments spanning the entire peptide chain of the T₁ enzyme (Figure 1) has now been completed.

The overall scheme of the present synthesis is based on the protected hydrazide approach⁶ and involved the synthesis of five subfragments (G₁–G₅) and their assembly by the azide procedure⁷ to form the tetracosapeptide amide G. Three subfragment combinations, *i.e.*, G₁G₂ + G₃, G₄ + G₅, and G₁ + G₂G₃ (Scheme I), were explored.

As in our previous syntheses of T₁ fragments, a

(5) K. Takahashi, *J. Biol. Chem.*, **240**, 4117 (1965).

(6) K. Hofmann, A. Lindenmann, M. Z. Magee, and N. H. Khan, *J. Amer. Chem. Soc.*, **74**, 470 (1952).

(7) J. Honzl and J. Rudinger, *Collect. Czech. Chem. Commun.*, **26**, 2333 (1961).